# Origin of magnetism and trend in $T_c$ in Cr-based double perovskites: Interplay of two driving mechanisms

Hena Das,[1] Prabuddha Sanyal,[1] T. Saha-Dasgupta,[1,*] and D. D. Sarma[2,†]
[1]*S.N. Bose National Centre for Basic Sciences, Kolkata 700098, India*
[2]*Solid State and Structural Chemistry Unit, Indian Institute of Science, Bangalore 560012, India*
(Received 11 January 2011; published 25 March 2011)

Employing first principles density functional calculations, together with solution of the low-energy, model Hamiltonian constructed in a first principles manner, we explored the origin of magnetism and the $T_c$ trend in Cr-based double perovskite series, $Sr_2CrB'O_6$ ($B'$ = W/Re/Os). Our study shows that the apparently puzzling $T_c$ trend in $Sr_2CrB'O_6$ ($B'$ = W/Re/Os) series can be understood in terms of the interplay of the hybridization driven mechanism and the superexchange mechanism.

DOI: 10.1103/PhysRevB.83.104418 PACS number(s): 75.50.−y, 71.20.Be

## I. INTRODUCTION

Oxides with high magnetic transition temperature ($T_c$) are important for technological advancement. A much discussed family of compounds in this connection are double perovskites, with a general formula $A_2BB'O_6$, $A$ = alkaline/rare-earth metals and $B/B'$ = transition metals. The observation[1] of large magnetoresistance with a fairly high ferromegnetic (FM) $T_c$ of about 410 K in $Sr_2FeMoO_6$ (SFMO) and its unusual origin of magnetism brought this family of compounds into the forefront of activity. Since then the question has been, can $T_c$ be boosted even further and if so, is there a systematic trend that can be observed and understood? Attempts have been made to dope SFMO with La to increase the $T_c$. Although some partial success has been achieved[2] following this path, $T_c$ was found to be boosted much more efficiently by moving to different choices of $B$ and $B'$ ions. The microscopic understanding of this increase, however, has not been achieved. A collection of measured transition temperatures seems to bear some correlation with the number of valence electrons among different double perovskite compounds (see Fig. 1 in Ref. 3). Focusing onto Cr-based series, namely $Sr_2CrB'O_6$ ($B'$ = W/Re/Os), the family with spectacularly high $T_c$, the measured $T_c$ shows a rapid increase as one moves from $Sr_2CrWO_6$ (SCWO)[4] with $T_c \approx 450$ K to $Sr_2CrReO_6$ (SCRO)[5] with $T_c \approx 620$ K to $Sr_2CrOsO_6$ (SCOO)[6] with $T_c \approx 725$ K. This rapid increase is curious considering the hybridization driven (HD) mechanism[7,8] of magnetism accepted so far for double perovskites, proposed in the context of SFMO, which would predict decrease rather than the increase.[9] Furthermore, the compound with the highest $T_c$ in this series, SCOO, is found to be an insulator making the issue even more interesting. Also, a distinction between others like SFMO and La doped SFMO and this series is a possible role of spin-orbit coupling (SOC) due to the presence of 5$d$ elements.

We have used density functional theory (DFT) based calculations, together with exact diagonalization of the Cr-$B'$ model Hamiltonian constructed in a first-principles-derived Wannier function basis, to probe this issue. Although a few DFT based studies[10] exist for individuals of these compounds, to the best of our knowledge, no comprehensive theoretical study exists to address the origin of the growing trend in $T_c$ within the series.

## II. METHODOLOGY

The DFT calculations were carried out using the plane wave pseudopotential method implemented within the Vienna Ab-initio Simulation Package (VASP).[11] The exchange-correlation functionals were approximated by generalized gradient approximation (GGA).[12] We have used projected augmented wave (PAW) potentials[13] and the kinetic energy cutoff for expansion of wave functions used was 450 eV. Reciprocal space integrations were carried out with a $k$-space mesh of 6×6×6. For extraction of a few-band, tight-binding Hamiltonian out of full GGA calculation, we carried out muffin-tin orbital (MTO) based NMTO-downfolding calculations.[14] The reliability of the calculations in two basis sets was cross checked.

## III. RESULTS

### A. Examination of basic electronic structure

In order to unravel the origin of magnetism in $Sr_2CrB'O_6$ series, let us first critically examine the electronic density of states (DOS) of these compounds. The left panel of Fig. 1 shows the DOS, as obtained in spin-polarized DFT calculations within GGA. The states close to Fermi level ($E_F$) are dominated by Cr and $B'$ $d$ states hybridized with O $p$ states, while the O $p$ dominated states separated from Cr and $B'$ $d$ dominated states occupy the energy range far below $E_F$, and the Sr $s$ and $d$ dominated state remains far above $E_F$. The $d$ states of Cr and the $B'$ ions are exchange split as well as crystal field split. The empty $B'$ $t_{2g}$ states in the up-spin channel appear in between the crystal field split Cr $t_{2g}$ and $e_g$ states, gapped from $E_F$, while the $B'$ states in the down-spin channel hybridized with Cr $t_{2g}$ states either cross the Fermi level, as in the case of W and Re compounds, or remain completely occupied, as in case of the Os compound. It is rather intriguing to notice that the hybridization between Cr $t_{2g}$ and $B'$ $t_{2g}$ in the down-spin channel progressively gets weakened in moving from W to Re to Os compounds. This may be appreciated by considering the Cr contribution measured with respect to the $B'$ contribution for the states in the down-spin channel close to $E_F$. For the W, Re, and Os compounds, it is found to be 66%, 16%, and 5%, respectively. This is caused by the gradual

 

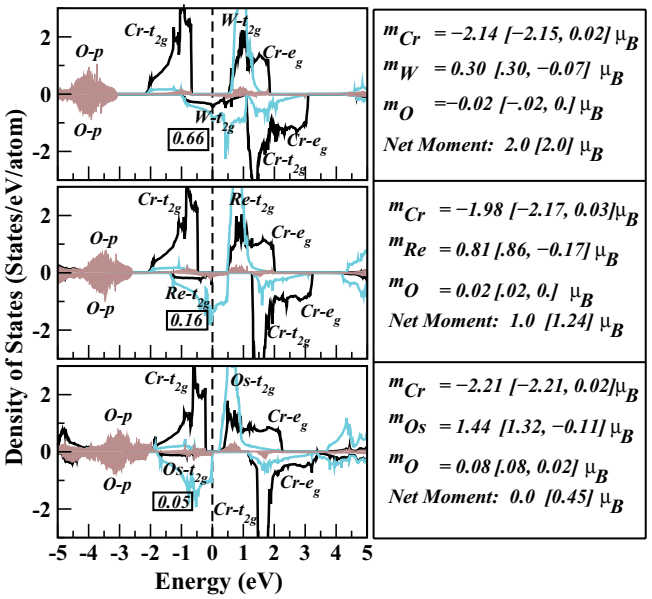


FIG. 1. (Color online) Left panels: GGA DOS projected onto Cr $d$ (black solid lines), $B'$ $d$ (red/gray solid lines), and O $p$ (shaded area). Zero of the energy is set at $E_F$. The numbers within the boxes indicate the Cr $t_{2g}$ contribution in the bands crossing $E_F$, with respect to that of $B'$. Right panel: Calculated net magnetic moment and magnetic moments at Cr, $B'$, and O sites. The numbers within the brackets denote the results of GGA + SO calculations, the first entry being the spin moment and the second entry being the orbital moment. From top to bottom, the plots correspond to SCWO, SCRO, and SCOO, respectively.

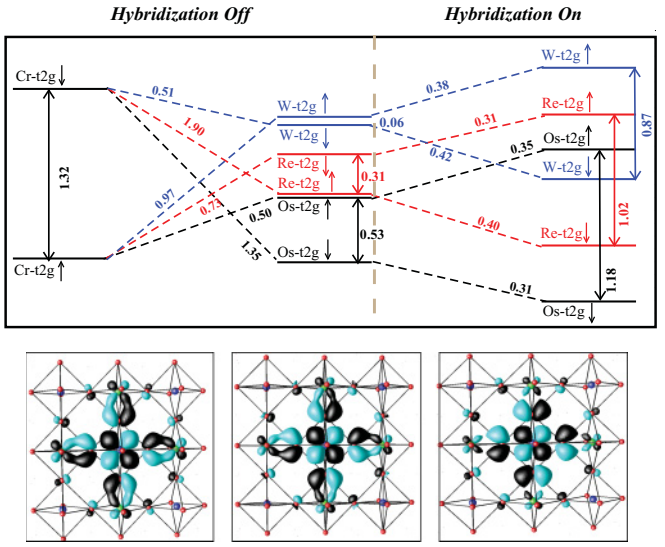


FIG. 2. (Color online) The energy level diagram (upper panel) and massively downfolded Wannier functions (lower panels) for $Sr_2CrB'O_6$ series. For Wannier function plots, constant value surfaces have been plotted with two oppositely signed lobes colored differently. From left to right in lower panel, the plots correspond to SCWO, SCRO, and SCOO, respectively. The numbers in the energy level diagram are in units of eV.

moving down of the $B'$ energy level, in moving from the left to the right of the periodic table across the same row (W → Re → Os), reflecting an increase in the ionic potential experienced by the 5$d$ electrons with an increase in nuclear charge. As discussed later, the hopping interaction connecting the Cr and $B'$ $t_{2g}$ states on the other hand remains similar across the series. Analyzing the DFT calculated magnetic moments, presented in the right panel of Fig. 1, we find the second interesting observation that the magnetic moment per electron at the $B'$ site, defined as $m/d$, where $m$ is the calculated moment and $d$ is the valence count at $B'$,[15] keeps growing from W to Re to Os. The increase in $m/d$ becomes even more evident taking into account the magnetic moment at the O site, which is small and points to the Cr moment for SCWO, and small (large) and points to the Re (Os) moment for SCRO (SCOO). This prompts us to conclude that there is a growing intrinsic moment that develops at the $B'$ site following the dehybridization effect between Cr and $B'$.

### B. NMTO downfolding calculations

In order to further analyze the findings of the electronic structure calculations, we have carried out NMTO downfolding calculations, which are engineered to define energy-selected, effective Wannier functions by integrating out degrees of freedom that are not of interest (*downfolding*). As a first step we downfolded O $p$ and Sr as well as Cr and $B'$ $e_g$ degrees of freedom. This defines an effective basis consisting of Cr $t_{2g}$ and $B'$ $t_{2g}$ states. In the second step, we applied massive downfolding, keeping only $B'$ $t_{2g}$ degrees of freedom active and downfolding all the rest including Cr $t_{2g}$ degrees of freedom. On-site matrix elements of the real space Hamiltonian defined in the Cr $t_{2g}$–$B'$ $t_{2g}$ basis and the massively downfolded basis give the energy level positions before and after switching on the hybridization between the Cr and $B'$ states, respectively. Figure 2 summarizes the results for the W, Re, and Os compounds. The energy levels in the left and right halves of the upper panel, demarcated with a vertical gray line, depict the energy level positions obtained out of the downfolded Cr $t_{2g}$–$B'$ $t_{2g}$ basis and the massively downfolded basis, respectively. The lower panels exhibit plots of the $t_{2g}$ ($xy$) Wannier function corresponding to the massively downfolded Hamiltonian in the down-spin channel. Examination of Fig. 2 brings out two aspects: First, the progressive dehybridization effect, as discussed in the context of DOS plots, is evident in the plots of Wannier functions. The central parts of the Wannier functions are shaped according to $B'$ $xy$ symmetry, and the tails of the Wannier functions sitting at neighboring sites are shaped according to O $p$ and Cr $t_{2g}$ symmetry. The tails reflecting the hybridization between the Cr $t_{2g}$ and $B'$ $t_{2g}$–O weaken as one moves from W to Re to Os compounds. As a consequence, the ratio of renormalized spin splitting to that of bare splitting at the $B'$ site reduces drastically from W (14.5) to Re (3.3) to Os (2.2). Second, considering the level splitting at the $B'$ site before switching on the hybridization, we find that while the splitting at W is negligibly small, confirming the nonmagnetic character of the $B'$ site, those for Re and Os are found to be ≈0.31 eV and ≈0.53 eV, respectively. These values are significantly larger compared to what one would have expected considering the $d^2$ valence in Re and the $d^3$ valence in Os compared to the $d^1$ valence in the case of W with 0.06 eV splitting, which

would have given rise to splittings of 0.12 eV and 0.18 eV, respectively. This confirms the presence of a growing intrinsic, local moment at the $B'$ site as one moves from W to Re to Os, driven by the dehybridization effect. The magnetism in Cr-B′ series, therefore, needs to be understood as an interplay of two mechanisms: the HD mechanism as operative in SFMO which causes renormalized, negative spin splitting within B′ states that appear in between the exchange split Cr $t_{2g}$ states, and the superexchange (SE) between the moment at the Cr site and the intrinsic moment at the $B'$ site, which would align the moments at the Cr and $B'$ sites antiparallely. For W, the intrinsic moment being negligible, the magnetism is entirely driven by the HD mechanism, while for the other extreme of Os, the hybridization effect is weak, SE having a rather large contribution. The presence of such intrinsic moment at the 5$d$ site is counterintuitive at first glance. Comparing the situation with the double perovskite $Sr_2ScReO_6$, for which the magnetism has been recently investigated,[16] Re was found to possess a rather small intrinsic moment of size 0.013 $\mu_B$. Our electronic structure calculations carried out for $Sr_2ScReO_6$ find also a similarly small moment (0.03 $\mu_B$). The unusual localized aspect of Re or Os, in case of the Cr based compounds therefore arises due to the relative positioning of the Cr and $B'$ energy levels, which narrows down the width of the $B'$ states substantially in the up-spin channel. The development of the intrinsic moment is thus helped by the delicate energy level structure responsible for the HD mechanism and would not have been present otherwise.

### C. Total energy calculations

The calculations discussed so far do not include SOC, which may be important. The numbers within the brackets in right panel of Fig. 1 show the individual spin and orbital moments as well as net moments as obtained in GGA + SO calculations. As expected, the orbital moments are large at the $B'$ site. Interestingly, we find while the net moment was zero for SCOO without SOC, it is the consideration of SOC that gives rise to a nonzero moment, due to the uncompensated orbital moment at the $B'$ site. Whether SOC has any influence on the trend within the $T_c$'s therefore needs to be explored. The interplay of two driving mechanisms in W-Re-Os series, however, makes it difficult to extract the magnetic exchanges as the energy difference between two specific magnetic configurations. The presence of a finite, intrinsic moment at the $B'$ site, as is the case for Re and Os compounds, makes the moment at the $B'$ site frustrated in an antiferromagnetic (AFM) configuration of Cr spins. The finite presence of the HD mechanism, on the other hand, disfavors stabilization of magnetic configurations with the majority of the $B$ spins aligned parallel to that of the moment at the $B'$ site. Admitting these difficulties, we carried out total energy calculations of the two possible spin configurations, one FM arrangement and another A-type AFM arrangement of Cr spins, where Cr spins between two adjacent planes are antiferromagnetically coupled, and are ferromagnetically coupled in plane. For the AFM calculations, the moment at the $B'$ site was found to be antiparallel (parallel) aligned to the spins of in-plane (out-of-plane) Cr sites which are four (two) in number. As expected, the energy differences between FM and AFM configurations are found to be positive for all cases proving FM arrangement of Cr spins to be the stable phase. The values of the energy difference are found to increase from W to Re systems (from 0.23 eV/formula unit to 0.25 eV/formula unit), and then decrease from Re to Os systems (from 0.25 eV/formula unit to 0.24 eV/formula unit). Although the introduction of the SO interaction changes the individual energy differences by about 0.03 eV, the trend remains unaltered. This indicates that although the presence of substantial SOC at the $B'$ site is important for producing the large magneto-optical signals,[17] it plays little role in setting up the trend in $T_c$. In order to examine the role of the missing correlation effect in GGA, we have also carried out LDA + $U$ calculations with a choice of $U$ value of 3 eV at the Cr site and 0.8 eV at the $B'$ site. The application of a larger $U$ at the Cr site and a relatively smaller one at the $B'$ sites, as expected from the relative bandwidths, were found to preserve the general conclusions intact with more localized character of $d$ states at the $B'$ site.

### D. Exact diagonalization study of model Hamiltonian

In view of the difficulty in stabilizing the appropriate excited state magnetic configuration, the stability of the FM arrangements of Cr spins may be measured as the energy difference between the FM spin configuration and the paramagnetic (PM) phase. The description of the PM phase needs consideration of different disordered spin configurations and averaging over a large number of them, which is almost impossible within the DFT framework. Such calculations are much easier to handle within a model Hamiltonian description. The model Hamiltonian describing the interplay of the HD and SE mechanisms may be written as

$$\begin{aligned} H = {} & \epsilon_{\mathrm{Cr}} \sum_{i\in B} f^{\dagger}_{i\sigma\alpha} f_{i\sigma\alpha} + \epsilon_{B'} \sum_{i\in B'} m^{\dagger}_{i\sigma\alpha} m_{i\sigma\alpha} \\ & - t_{CB'} \sum_{\langle ij\rangle\sigma,\alpha} f^{\dagger}_{i\sigma,\alpha} m_{j\sigma,\alpha} - t_{B'B'} \sum_{\langle ij\rangle\sigma,\alpha} m^{\dagger}_{i\sigma,\alpha} m_{j\sigma,\alpha} \\ & - t_{CC} \sum_{\langle ij\rangle\sigma,\alpha} f^{\dagger}_{i\sigma,\alpha} f_{j\sigma,\alpha} + J \sum_{i\in Cr} \mathbf{S}_i \cdot f^{\dagger}_{i\alpha} \vec{\sigma}_{\alpha\beta} f_{i\beta} \\ & + J_2 \sum_{i\in \mathrm{Cr},\, j\in B} \mathbf{S}_i \cdot \mathbf{s}_j, \end{aligned}$$

where the $f$'s and $m$'s refer to the Cr $t_{2g}$ and $B'$ $t_{2g}$ degrees of freedoms. $t_{CB'}$, $t_{B'B'}$, and $t_{CC}$ represent the nearest neighbor Cr-$B'$ and second nearest neighbor $B'$-$B'$ and Cr-Cr hoppings, respectively. $\sigma$ is the spin index and $\alpha$ is the orbital index that spans the $t_{2g}$ manifold. The difference between the ionic levels, $\Delta = \epsilon_{\mathrm{Cr}} - \epsilon_{B'}$, defines the on-site energy difference between the Cr $t_{2g}$ and $B'$ $t_{2g}$ levels. $s_j$ is the intrinsic moment at the $B'$ site. The first six terms of the Hamiltonian represent the HD mechanism, which consists of a large core spin at the Cr site ($S_i$) and the coupling between the core spin and the itinerant electron delocalized over the Cr-$B'$ network. Variants of this part has been considered by several authors[18–20] in the context of SFMO. The last term represents the SE mechanism, which consists of coupling between Cr spin and the intrinsic moment at the $B'$ site. The parameters of the model Hamiltonian are extracted out of DFT calculations through the NMTO downfolding technique of constructing

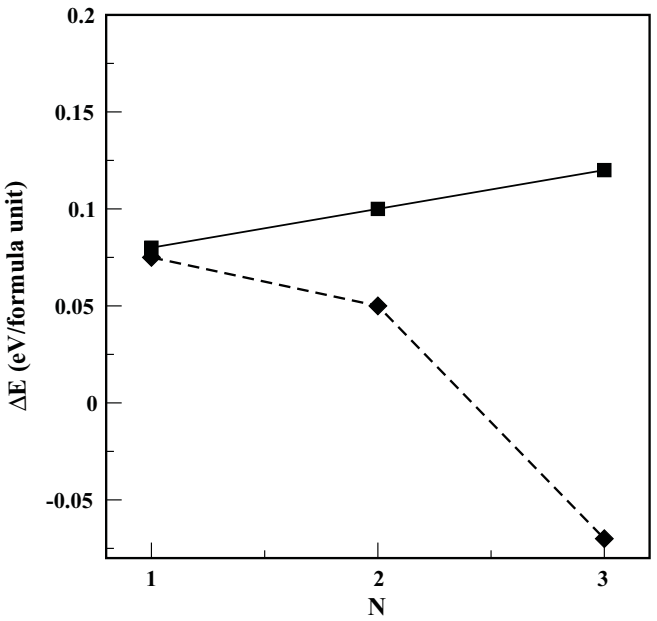


FIG. 3. PM-FM energy differences plotted as a function of valence electron count, as obtained in exact diagonalization calculation. The diamond (square) symbols connected by dashed (solid) lines correspond to calculations corresponding to the Hamiltonian without (with) the $J_2$ term.

the real space Hamiltonian in the basis of the effective Cr $t_{2g}$ and $B'$ $t_{2g}$ degrees of freedom. The $t_{CB'}$, $t_{B'B'}$, and $t_{CC}$ hoppings are found to be $-0.35$ eV, $-0.12$ eV, and $-0.08$ eV, respectively, with little variation within the W-Re-Os series. The $\Delta$'s show a varying trend within the W-Re-Os series ($\Delta^{W} = -0.66$ eV, $\Delta^{Re} = 0.03$ eV, and $\Delta^{Os} = 0.26$ eV). The parameters involving $J$ and $J_2$ were obtained from the spin splitting at the Cr site and the extra splitting observed at the $B'$ site as compared to that expected from the electron filling effect and the splitting for the W compound.

The constructed model is then solved using exact diagonalization on a lattice of dimensions $8 \times 8 \times 8$. Calculations have been carried out as well for lattices of size $4 \times 4 \times 4$ and $6 \times 6 \times 6$. The trend is found to be the same as presented for $8 \times 8 \times 8$. Exact diagonalization was first carried out considering the $B'$ site to be totally nonmagnetic, i.e., setting the last term to zero, which boils down to the same underlying model Hamiltonian as that of SFMO. The energy difference between the PM and FM is found to decrease with increasing number of valence electrons, as shown by the diamond symbols in Fig. 3. This is exactly the same trend as found in a recent calculation on La doped SFMO,[21,22] as well as in Ref. 9 with FM getting destabilized with increase of valence electrons. This trend of suppression of $T_c$ upon increasing valence electron count is further amplified due to change in $\Delta$ within the Cr-$B'$ series. This variation in $\Delta$ in the present series is in contrast to the prescription given in Ref. 9 to achieve high $T_c$. Upon reaching a valence electron count equal to 3 which corresponds to the Os compound, FM becomes totally unstable, reflected in the negative sign of the energy difference. We note a rather rapid decrease in moving from the $N = 2$ case to the $N = 3$ case. This may reflect the special situation of Os compound, with Cr $t_{2g}^3$–$B'$ $t_{2g}^3$ configuration, an ideal super-exchange situation with insulating solution, that adds on to the general trend. The situation gets dramatically changed upon inclusion of the growing localized magnetic nature of the $B'$ site, as shown by the square symbols in Fig. 3. Considering the $J_2$ values, as obtained in GGA calculations, we find that the PM and FM energy difference recovers the correct trend in moving from W to Re to Os, as has been observed experimentally. Mapping the PM and FM energy difference to the mean field $T_c$, one obtains values 870 K, 1160 K, and 1450 K for the W, Re, and Os compounds, respectively. Although the values are overestimated compared to experimental values, presumably due to the finite size effect of the exact diagonalization calculation and the mean field formula, the trend is very well reproduced with $T_c^{Re}/T_c^{W} = 1.33$ and $T_c^{Os}/T_c^{Re} = 1.25$, compared to experimental estimates of 1.38 and 1.17, respectively.[4–6]

## IV. CONCLUSION AND DISCUSSION

In conclusion, we have studied the counterintuitive $T_c$ trend in Cr based double perovskites, $Sr_2CrB'O_6$ ($B' = W/Re/Os$). Analysis of the electronic and magnetic properties shows that the progressive enhancement of $T_c$ across the $5d$ series should be understood as the interplay of two driving mechanisms: the HD mechanism responsible for the negative spin splitting at the $B'$ site as in SFMO, and the SE mechanism. The HD mechanism gets weaker as one moves along the series from W to Re to Os, due to the increased energy level separation of $B'$ from Cr. SE, on the other hand, gets stronger in moving from SCWO to SCRO to SCOO due to the presence of growing intrinsic moment at the $B'$ site, following the dehybridization effect. The observed uncompensated moment in SCOO arises due to the presence of SO. SCOO, in that sense, should be thought of as a ferrimagnet rather than a ferromagnet. With this, we demystify the puzzling $T_c$ trend in the Cr-$B'$ double perovskite series.

## ACKNOWLEDGMENTS

T.S.D. and D.D.S. acknowledge support of DST, Swarnajayanti, and J. C. Bose fellowships. T.S.D. gratefully acknowledges discussion with L. Alff.

*tanusri@bose.res.in
†sarma.dd@gmail.com

[1] K.-I. Kobayashi, T. Kimura, H. Sawada, K. Terakura, and Y. Tokura, Nature (London) **395**, 677 (1998).

[2] J. Navarro, J. Fontcuberta, M. Izquierdo, J. Avila, and M. C. Asensio, Phys. Rev. B **69**, 115101 (2004); C. Frontera, D. Rubía, J. Navarroa, J. L. García-Muñoza, C. Ritterb, and J. Fontcuberta, Physica B **350**, e285 (2004).

[3]Tapas Kumar Mandal, Claudia Felser, Martha Greenblatt, and Jürgen Kübler, Phys. Rev. B **78**, 134431 (2008).
[4]J. B. Philipp *et al.*, Phys. Rev. B **68**, 144431 (2003).
[5]H. Kato, T. Okuda, Y. Okimoto, Y. Tomioka, Y. Takenoya, A. Ohkubo, M. Kawasaki, and Y. Tokura, App. Phys. Lett **81**, 328 (2002).
[6]Y. Krockenberger, K. Mogare, M. Reehuis, M. Tovar, M. Jansen, G. Vaitheeswaran, V. Kanchana, F. Bultmark, A. Delin, F. Wilhelm, A. Rogalev, A. Winkler, and L. Alff, Phys. Rev. B **75**, 020404 (2007).
[7]D. D. Sarma, Priya Mahadevan, T. Saha-Dasgupta, Sugata Ray, and Ashwani Kumar, Phys. Rev. Lett. **85**, 2549 (2000).
[8]J. Kanamori and K. Terakura, J. Phys. Soc. Jpn. **70**, 1433 (2001).
[9]A. Chattopadhyay and A. J. Millis, Phys. Rev. B **64**, 024424 (2001).
[10]H. T. Jeng and G. Y. Guo, Phys. Rev. B **67**, 094438 (2003); G. Vaitheeswaran *et al.*, Appl. Phys. Lett. **86**, 032513 (2005); K. W. Lee and W. Pickett, Phys. Rev. B **77**, 115101 (2008).
[11]G. Kresse and J. Furthmüller, Phys. Rev. B **54**, 11169 (1996).
[12]J. P. Perdew, J. A. Chevary, S. H. Vosko, K. A. Jackson, M. R. Pederson, D. J. Singh, and C. Fiolhais, Phys. Rev. B **48**, 4978 (1996).
[13]P. E. Blöchl, Phys. Rev. B **50**, 17953 (1994).
[14]O. K. Andersen and T. Saha-Dasgupta, Phys. Rev. B **62**, R16219 (2000).
[15]The nominal $5^+$ valence state corresponds to the $5d^1$, $5d^2$, and $5d^3$ configuration of W, Re, and Os, respectively.
[16]A. Winkler, N. Narayanan, D. Mikhailova, K. G. Bramnik, H. Ehrenberg, H. Fuess, G. Vaitheeswaran, V. Kanchana, F. Wilhelm, A. Rogalev, A. Kolchinskaya, and L. Alff, New J. Phys. **11**, 073047 (2009).
[17]H. Das, M. De-Raychaudhury, and T. Saha-dasgupta, Appl. Phys. Lett. **92**, 201912 (2008).
[18]J. L. Alonso, L. A. Fernández, F. Guinea, F. Lesmes, and V. Martín-Mayor, Phys. Rev. B **67**, 214423 (2003).
[19]O. Navarro, E. Carvajal, B. Aguilar, and M. Avignon, Physica B **384**, 110 (2006).
[20]L. Brey, M. J. Calderón, S. Das Sarma, and F. Guinea, Phys. Rev. B **74**, 094429 (2006).
[21]P. Sanyal, H. Das, and T. Saha-Dasgupta, Phys. Rev. B **80**, 224412 (2009).
[22]The experimental observation of increase of $T_c$ upon La doping in SFMO may be rationalized in terms of the increase of the antisite disorder as predicted in Ref. 18.